https://doi.org/10.5194/esurf-2021-41
Preprint. Discussion started: 26 May 2021

Earth Surface Dynamics Discussions
Open Access
EGU

Temporal changes in the debris flow threshold under the effects of ground freezing and sediment storage on Mt. Fuji

Fumitoshi Imaizumi[1], Atsushi Ikeda[2], Kazuki Yamamoto[3], Okihiro Ohsaka[4]

[1]Faculty of Agriculture, Shizuoka University, Shizuoka, 422-8429, Japan
[2]Faculty of Life and Environmental Sciences, University of Tsukuba, 305-8572, Japan
[3]Bureau of Economic Affairs, Shizuoka city office, Shizuoka, 422-8429, Japan
[4]Shizuoka Professional University of Agriculture, Japan, 424-8701

Correspondence to: Fumitoshi Imaizumi (imaizumi@shizuoka.ac.jp)

Abstract. Debris flows are one of the most destructive sediment transport processes in mountainous areas because of their large volume, high velocity, and kinematic energy. Debris flow activity varies over time and is affected by changes in hydrogeomorphic processes in the initiation zone. To clarify temporal changes of debris flow activities in cold regions, the rainfall threshold for the debris flow occurrence was evaluated in Osawa failure at a high elevation on Mt. Fuji, Japan. We conducted field monitoring of the ground temperature near a debris flow initiation zone to estimate the presence or absence of seasonally frozen ground during historical rainfall events. The effects of ground freezing and the accumulation of channel deposits on the rainfall threshold for debris flow occurrence were analyzed using rainfall records and annual changes in the volume of channel deposits since 1969. Statistical analyses showed that the intensity-duration threshold during frozen periods was clearly lower than that during unfrozen periods. A comparison of maximum hourly rainfall intensity and total rainfall also showed that debris flows during frozen periods were triggered by a smaller magnitude of rainfall than during unfrozen periods. Decreases in the infiltration rate due to the formation of frozen ground likely facilitated the generation of overland flow, triggering debris flows. During unfrozen periods, the rainfall threshold was higher when the volume of channel deposits was larger. Increases in the water content in channel deposits caused by the infiltration of rainfall is likely important for the debris flow occurrence during unfrozen periods. The results suggest that the occurrence of frozen ground and the sediment storage volume need to be monitored and estimated for better debris flow disaster mitigation in cold regions.

1 Introduction

Debris flows are one of the most destructive sediment transport processes in mountain areas because of their large volume and high velocity and kinematic energy (Scott et al., 2004; Theule et al., 2018; Song et al., 2019). Debris flow risks are increasing in cold mountainous regions under climate change due to changes in hydrological processes on hillslopes, increases in the magnitude of rainfall events, and those in sediment supply activity in their initiation zones (Stoffel and Huggel, 2012; Stoffel et al., 2014). Because debris flows are usually triggered by heavy rainfall events (Scott et al., 2004; Sidle and Chigira, 2004;

https://doi.org/10.5194/esurf-2021-41
Preprint. Discussion started: 26 May 2021

Dowling and Santi, 2014; Zhang et al., 2019), estimation of the rainfall thresholds triggering debris flows is essential for debris flow hazard mitigation measures, such as the installation of early warning systems (Pan et al., 2018; Hürlimann et al., 2019).

Many studies have attempted to determine rainfall thresholds by analyzing rainfall records in periods with and without a debris flow (e.g., Cannon et al., 2011; Hürlimann et al., 2019). The intensity-duration (ID) threshold is one of the most commonly used rainfall thresholds (Caine, 1980; Guzzetti et al., 2008; Staley et al., 2012; Zhou and Tang, 2014). Other factors, such as cumulative rainfall depth and the return time of rainfall, have also been used to estimate rainfall thresholds (Fiorillo and Wilson, 2004; Imaizumi et al., 2006). Although many studies have calculated a single rainfall threshold for each torrent and region, the threshold varies with time and is affected by changes in hydrological processes and the volume of debris flow material (Jakob et al., 2005; Schlunegger et al., 2009; Chen et al., 2012; Theule et al., 2012). Therefore, temporal changes in the rainfall threshold need to be understood to evaluate future risks of debris flows under climate change.

Debris flow activity is controlled by hydrological characteristics on hillslopes and debris flow material (i.e., channel deposits and talus slopes) in debris flow initiation zones (Bovis and Dagg, 1988; Staley et al., 2014; Loye et al., 2016). Wildfires decrease the infiltration rate of rainfall into the ground, resulting in the generation of overland flow that leads to debris flows (Cannon et al., 2001; Shakesby and Doerr, 2006; Ebel et al., 2012; Staley et al., 2014). The hydraulic conductivity of debris flow material also controls the initiation of debris flows (Bovis and Dagg, 1988). Ground freezing changes hydrological processes in watersheds, with the infiltration rate generally low in periods with a frozen soil layer (Blackburn et al., 1990; Iwata et al., 2010). Thus, the discharge of shallow runoff during the frozen period is higher than during the unfrozen period (Shanley and Chalmers, 1999; Coles and McDonell, 2018). However, the effect of ground freezing on the rainfall threshold of debris flow remains poorly understood.

The volume of debris flow material in the initiation zones of debris flow is controlled by the sediment supply from hillslopes and the evacuation of sediment by debris flows and fluvial processes (Imaizumi et al., 2006; Berger et al., 2011a; Theule et al., 2012; Imaizumi et al., 2019). Debris flow frequency is generally high in torrents with high sediment supply activity (May, 2002; Jakob et al., 2005). Bovis and Jakob (1999) classified debris flow basins into weathering-limited basins, which require a long sediment recharge period for the occurrence of a debris flow, and transport-limited basins, in which the debris flow occurrence is primarily controlled by hydroclimatic events. These studies imply that the volume of debris flow material in the watershed needs to be interpreted to improve the accuracy of debris flow prediction.

Mount Fuji, which is the most famous mountain of Japan, has frequently experienced severe debris flow disasters, as well as slush avalanches, which are mixtures of water and snow that erode large amounts of sediment as they move downstream (Hanaoka et al., 2007). Sediment accumulated in gully bottoms, which is eroded by overland flow during rainfall events, is the main source of debris flow material. Many disasters around Mt. Fuji have occurred in spring and late autumn, despite precipitation in those seasons being lower than in summer and early autumn (Hanaoka et al., 2007). Although previous interpretations have implied that seasonal ground freezing affects temporal changes in the rainfall threshold of debris flow (Anma, 2007), this has not been supported by quantitative analyses due to the lack of field monitoring data. On Mt. Fuji, the

https://doi.org/10.5194/esurf-2021-41
Preprint. Discussion started: 26 May 2021


Earth Surface Dynamics Discussions Open Access EGU

sediment storage volume in debris flow torrents has also changed over time because of the sediment supply from hillslopes and the evacuation of sediment by debris flows (Hanaoka et al., 2007).

The overall aim of this study was to clarify temporal changes in the rainfall threshold for the debris flow occurence in a cold region under the effects of seasonal ground freezing and changes in the sediment storage volume. We conducted field monitoring of ground temperatures on Mt. Fuji to estimate the ground freezing conditions during historical rainfall events that triggered or did not trigger debris flows and slush avalanches. The specific objectives of the study were to estimate periods of ground freezing over 50 years using an empirical model based on field monitoring, calculate the rainfall thresholds in periods with and without frozen ground given changes in the sediment storage volume, and understand the hydrological processes triggering debris flows in relation to the formation of frozen ground and the volume of debris flow material.

2 Study site

Osawa failure, which is a huge gully (length 2.1 km, width 500 m, and depth 150 m), is the most active debris flow torrent on Mt. Fuji. The Osawa failure is located on the western slope of Mt. Fuji (Figs. 1a, 1b), where a westerly wind dominates. Results of age determination using C^{14} indicated that this gully started to form circa 3,000 years ago (Iwatsuka and Machida, 1962). The Osawa failure increased in size following a catastrophic failure circa 1,000 years ago (Hanaoka et al., 2007). The total volume of sediment derived from the gully is estimated to be 75,000,000 m^3. The west side of Mt. Fuji is underlain by an alternation of scoria and basaltic lava, whereas thick tephra layers occur on the east side (Miyaji, 1998). Unconsolidated scoria layers have been actively eroded by freeze-thaw activity, overland flows, and strong winds. As the erosion of basal scoria layers proceeds, the lava outcrop becomes unstable due to overhanging, resulting in episodic failure of the outcrop of up to 30 m in thickness. Between 1970 to 2004, the estimated total volume of sediment evacuated from the Osawa failure was 5,020,000 m^3 (Hanaoka et al., 2007).

The Osawa failure has a cold climate due to its high elevation. The monthly average air temperature around the debris flow initiation zone (3,200 m a.s.l.) is lower than 0°C from November to April (Fig. 2). The maximum daily air temperature is also below 0°C from November to April, facilitating the development of seasonally frozen ground. The average annual precipitation from 2010 to 2019 was 2,737 mm. Heavy rainfall (>100 mm) occurs during the “Baiu” rainy season (i.e., monsoon season from June to July) and during typhoon crossings (August to October). Precipitation in winter (December to February) accounts for only 8% of the annual precipitation.

In the Osawa failure, the slope gradients of the scoria and lava layers are 35–50° and 40–90°, respectively. Talus slopes, with a slope gradient of 35–40°, are distributed at the foot of the hillslopes. Most parts of the channel are generally covered by channel deposits, which are the main sources of debris flow material (Figs. 1c, 1d). The channel gradient in the gully ranges from 20° (the lower part of the Osawa failure) to 35° (channel head). Debris flows and slush avalanches in the Osawa failure generally run down Osawa Creek to the Osawa alluvial fan, which is located approximately 6 km west of the gully. Some small-scale debris flows terminate in the Osawa failure and the channel sections between the gully and alluvial fan.

https://doi.org/10.5194/esurf-2021-41
Preprint. Discussion started: 26 May 2021

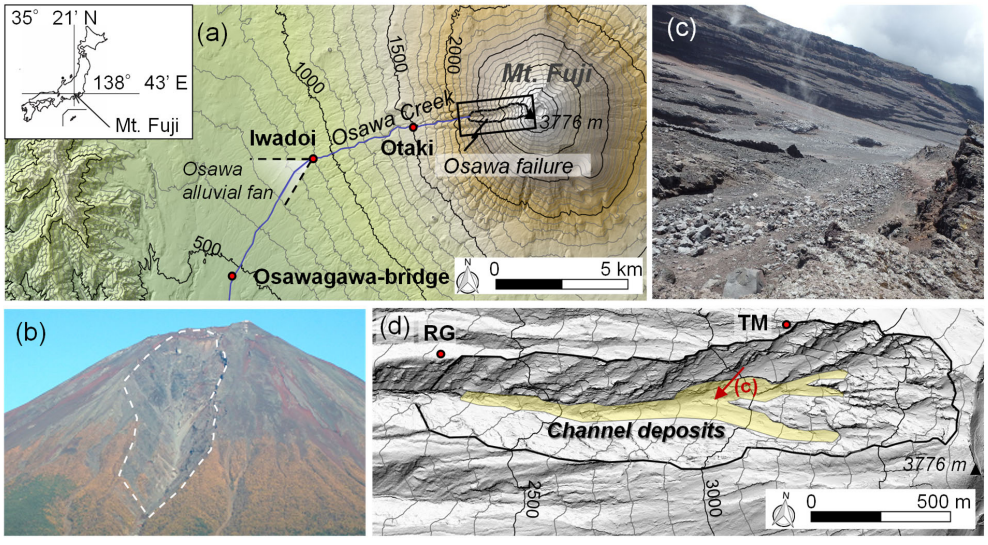

Figure 1: Topographic map and photographs of the Osawa failure. (a) Topographic map of the area around the Osawa failure and Osawa Creek. The area shown in (d) is located within the black-outlined box. (b) Full view of Mt. Fuji. The location of the Osawa failure is indicated by the white dashed line. (c) Channel deposits in the Osawa failure. The location where this photograph was taken is indicated by the red arrow in (d). (d) Topographic map of the area around the Osawa failure. RG and TM indicate the locations of a rain gauge and ground temperature sensors, respectively.

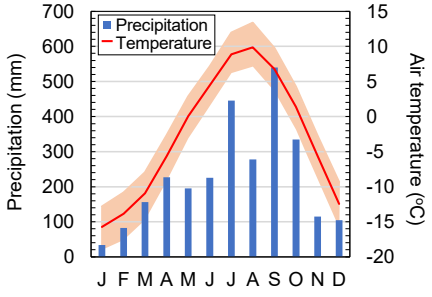

Figure 2: Average monthly precipitation at 2,330 m a.s.l. (RG in Fig. 1d) and air temperature around the debris flow initiation zone (3,200 m a.s.l.) in the Osawa failure from 2010 to 2019. Air temperature around the debris flow initiation zone was estimated from that recorded at the summit station (3,775 m a.s.l.) and the lapse rate (0.55). Solid air temperature curve indicates monthly average temperature, while the upper and lower bounds of the shaded area indicate the average daily maximum and minimum temperatures, respectively, in each month.

https://doi.org/10.5194/esurf-2021-41
Preprint. Discussion started: 26 May 2021

The Ministry of Land, Infrastructure, Transport, and Tourism (MLIT) has been monitoring debris flows and slush avalanches in the Osawa failure and Osawa Creek since 1969. The runout timing of previous debris flows was observed with video cameras and water level gauges at Osawagawa Bridge Observatory (490 m a.s.l.) and Iwadoi Observatory (900 m a.s.l.), as well as with wire sensors and video cameras at Otaki Observatory (1,500 m a.s.l., Fig. 1a). Some debris flows were just monitored at one or two observatories because of the absence of monitoring devices, problems encountered during monitoring, or the short travel distance of the debris flows. The MLIT has also distinguished slush avalanches from debris flows based on field surveys just after each event and the presence or absence of snow in the flow as captured by video cameras. A total of 35 debris flows and eight slush avalanches were monitored from 1969 to 2019 (Fuji Sabo Office, 2017; Fuji Sabo Office, 2020). The maximum total discharge of the debris flows, which was estimated with a video camera, ultrasonic water level gauge, and Doppler flow-velocity sensor at Iwadoi observatory, was 3×10^5 m^3 (Fuji Sabo Office, 2017).

3 Methodology

3.1 Ground temperature monitoring

A depth profile of the ground temperature was obtained at an elevation of 3,220 m a.s.l. along the northern boundary of the Osawa failure (TM in Fig. 1d). The elevation of the monitoring point was selected based on the known initiation points of many debris flows, which were determined in an analysis of aerial photographs and airborne Light Detection and Ranging (LiDAR) digital elevation models (DEMs). A 2-m-deep hole was drilled in welded scoria. Then, temperature sensors (TMC-HD, Onset) were installed at 10 different depths (ground surface, 0.1, 0.25, 0.5, 0.75, 1.0, 1.25, 1.5, 1.75, and 2 m vertically) and connected to data loggers (U12-008, Onset). Errors in temperature measurement after calibration of the sensors were within ± 0.1°C. Monitoring was conducted from September 30, 2017 to September 17, 2019, with temperature recorded at intervals of 1 hr. The sensor at the ground surface was covered by pebbles to match its albedo to that of the natural ground surface.

The occurrence of diurnal freeze-thaw activity and the formation of seasonally frozen ground were determined based on observed ground temperature data. The period with diurnal freeze-thaw activity was determined to be the period during which the ground surface temperature rose above and fell below 0°C within 1 day, whereas the period with seasonal ground freezing was determined to be the period during which the ground temperature was equal to or below 0°C over multiple days.

3.2 Estimation of frozen periods

To estimate the presence or absence of seasonally frozen ground during rainfall events before the monitoring of ground temperature began, the downward progress of the freezing and thawing fronts at the debris flow initiation zone since 1969 was estimated using air temperature records for the summit of Mt. Fuji (3,775 m a.s.l.), which were provided by the Japan Meteorological Agency (JMA). Because the ground-freezing period is spatially variable and affected by slope orientation, elevation, and snow distribution (e.g., Bayard et al., 2005; Kneisel et al., 2015), it is difficult to precisely estimate the frozen

https://doi.org/10.5194/esurf-2021-41
Preprint. Discussion started: 26 May 2021

period at an exact debris flow initiation point, which differs among debris flow events inside the Osawa failure. Therefore, we estimated the frozen period at TM using the simple degree-day method to conduct an initial evaluation of the effect of ground freezing on the debris flow occurence.

First, the ground surface temperature at the debris flow initiation zone was estimated using a regression equation for the relationship between air temperature at the summit station and the monitored ground surface temperature from September 30, 2017 to September 17, 2019 (R^2=0.94). Then, the downward progress of the freezing and thawing fronts was obtained from freezing degree days and thawing degree days, respectively, which were calculated from the estimated ground surface temperature (Yamazaki, 1998; Miao et al., 2019; Walvoord et al., 2019) as follows:

$$D_f = c_f(-\sum T)^{1/2}, T < 0 \quad (1)$$

$$D_m = c_m(\sum T)^{1/2}, T > 0 \quad (2)$$

where D_f is the depth of the freezing front, T is the daily average temperature, D_m is the depth of the thawing front, and c_f and c_m are coefficients. The coefficients c_f and c_m, which reflect temporal changes in the freezing and thawing depths as calculated from monitoring data, were used for the estimation of the freezing and thawing fronts before field monitoring began.

Air temperature at the Fuji City meteorological station (20 km south of the Osawa failure), which is also maintained by the JMA, was used to estimate the ground temperature in the period for which data from the summit station were unavailable (0.9% of 1969–2019), although the elevation of this station (66 m a.s.l.) is much lower than that of the debris flow initiation zone. The regression equation for the relationship between the air temperature at the Fuji City station and ground surface temperature at the debris flow initiation zone (TM) was used to estimate the freezing and thawing lines in a depth-time graph (R^2=0.93). In this study, the periods between freezing and thawing lines are referred to as frozen periods, whereas the periods between thawing and subsequent freezing lines are referred to as unfrozen periods.

Except for the gully bottom, snow cover in the Osawa failure is generally shallow or absent, even in mid-winter, due to its slope orientation (windward side of Mt. Fuji), steep topography, and low precipitation (Fig. 2). Therefore, we did not consider snow cover to estimate the freezing and thawing lines.

3.3 Rainfall monitoring

From May 1, 1969, the MLIT has observed precipitation at 2,330 m a.s.l. using a tipping-bucket rain gauge, with a precision of 1 mm, close to the Osawa failure. The rain gauge, which has an internal heating system, can also monitor winter precipitation. The observation of precipitation was occasionally interrupted by problems with the monitoring system in winter (mainly from December to April) until 2012, because of difficulties with maintenance. Hence, we could not obtain precipitation data associated with seven debris flows and one slush avalanche.

https://doi.org/10.5194/esurf-2021-41
Preprint. Discussion started: 26 May 2021

Earth Surface Dynamics Discussions
Open Access
EGU

Rainfall thresholds appropriately separating rainfall events with and without debris flows were determined by calculating the critical successful index (CSI) using the following equation (e.g., Liao et al., 2011; Formetta et al., 2016; Staley et al., 2017):

$$\mathrm{CSI} = \frac{tp}{t_p + fp + fn} \quad (3)$$

where *tp* is the number of true positive events, *fp* is the number of false positive events, and *fn* is the number of false negative events. In this study, the ID threshold, a widely used concept (e.g., Guzzetti et al., 2008; Hürlimann et al., 2019), was employed to determine the importance of intensity and duration on the debris flow occurence. The rainfall threshold was also obtained by comparing the maximum hourly intensity and total rainfall to further improve our understanding of the debris flow initiation mechanism. Appropriate rainfall thresholds were determined under various conditions in the debris flow initiation zone, such as the presence or absence of a frozen layer and large or small volumes of sediment storage. Debris flows and slush avalanches were likely to occur in the period with and without a snowpack in their initiation zones, respectively. We did not distinguish between debris flows and slush avalanches to obtain rainfall thresholds, because the presence or absence of a snowpack during rainfall events was unclear, especially during events without significant sediment transfer. Rainfall events with a total rainfall <10 mm were not analyzed in this study, because they appeared unrelated to the occurrence of debris flows and slush avalanches. The time period used to separate different rainfall events was set to 24 h, which was longer than in many other studies (e.g., Bezak et al., 2016; Imaizumi et al., 2017). This was because the time required for flood concentration in the Osawa failure is likely longer than for many other debris flow torrents due to the large catchment area.

3.4 Changes in the volume of channel deposits

The MLIT measured the topography of the entire Osawa failure annually using aerial photogrammetry from 1970 to 2006 and airborne LiDAR from 2007 to 2019 (Fuji Sabo Office, 2017, 2020). The measurements were mainly conducted from September to October, when weather conditions were stable and there was no snowpack. In the period prior to 2007, DEMs with a grid size of 10 × 10 m or 5 × 10 m were constructed annually via photogrammetry using monochromatic and color aerial photographs, with scales of 1/3,000 to 1/10,000. The horizontal and vertical errors of the control points obtained at feature intersections were in the range of 0.15 to 0.30 m.

Since 2007, DEMs with a grid size of 0.5 to 1.0 m have been constructed from point clouds obtained via airborne LiDAR scanning, with a point density of 2.25 to 4.0 points m^{-2}. The accuracy of the measurements as determined by a comparison with ground control points on the alluvial fan was <0.1 m. The root mean square error of the elevation data between adjacent flight courses was also <0.1 m. Errors in the measurements were likely larger on steeper terrain, especially at the basalt outcrops in the Osawa failure.

https://doi.org/10.5194/esurf-2021-41
Preprint. Discussion started: 26 May 2021

Earth Surface Dynamics Discussions
Open Access
EGU

Fiji Sabo Office (2020) estimated the volume of channel deposits inside the Osawa failure using a DEM in November 2000, when channel deposits were absent due to evacuation by debris flows, thus determining the base topography of the channel bed (Fig. 3). In the 1974–1975, 1979–1980, and 1998–1999 periods, when topography was measured using aerial photographs, the loss of a large volume of channel deposits (>100,000 m^3) was estimated despite there being no debris flow signals at the Otaki, Iwadoi, and Osawagawa Bridge observatories. Errors in the estimation of sediment volume as well as the occurrence of debris flows terminating in the section between the Osawa failure and the observatories possibly affected the evaluated loss of channel deposits. Hence, our analysis of the volume of channel deposits contains some inherent errors for the period in which data were obtained using aerial photography surveys.

In this study, we obtained rainfall thresholds for two volume classes of channel deposits: ≥350,000 m^3 and <350,000 m^3. The boundary of the two classes was set to 350,000 m^3 to ensure that a statistically sufficient number of debris flow events could be allocated to both volume classes.

Table 1: Dates of airborne LiDAR measurements

Date of measurement	Grid size (m)
October 4 to November 6, 2008	0.5
October 11 to October 18, 2009	0.5
October 2 to November 2, 2010	0.5
June 4 to June 22, 2011	0.5
September 28 to September 29, 2011	0.5
November 23 to November 27, 2011	0.5
September 26 to September 29, 2012	0.5
October 8 to November 14, 2013	0.5
September 22 to October 27, 2014	0.5
October 6 to October 18, 2015	0.5
October 4 to October 21, 2016	0.5
August 9, 2017	0.5
August 1 to August 22, 2018	1.0
August 4 to August 6, 2019	1.0

https://doi.org/10.5194/esurf-2021-41
Preprint. Discussion started: 26 May 2021

Earth Surface Dynamics Discussions
Open Access
EGU

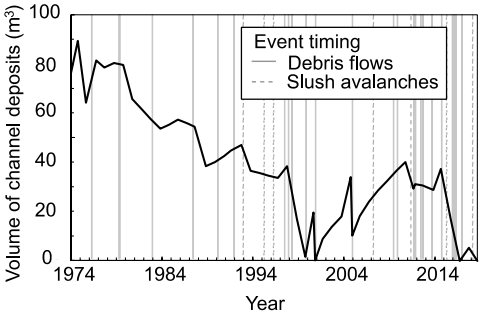

Figure 3: Temporal changes in the volume of channel deposits in the Osawa failure (original data from Fuji Sabo Office, 2020).

4 Results

4.1 Changes in ground temperature

In the shallower part of the ground (i.e., ≤0.25 m deep), diurnal freeze-thaw activity was frequently observed in autumn and spring, when the diurnal amplitude of the ground surface temperature was evident, whereas seasonally frozen ground was observed in winter (Figs. 4 and 5). At depths between 0.25 to 1.25 m, seasonally frozen ground occurred over long periods up to four months (Fig. 5). The ground below 1.75 m was not frozen in both the 2017–2018 and 2018–2019 frozen periods. Temporal patterns in the ground temperature were different between the 2017–2018 and 2018–2019 frozen periods (Fig. 4). In 2017–2018, ground temperature above a depth of 1.5 m rapidly increased during a heavy rainfall event on March 5 (total rainfall and maximum hourly rainfall of 89 mm and 18 mm h^{-1}, respectively), which triggered a slush avalanche. Although the seasonally frozen layer was retained for more than 1 month after the rainfall event, the ground temperature at a depth >0.5 m did not fall much below 0°C. In spring 2019, when heavy rainfall events were not observed, the ground temperature below 0.5 m was lower than that in spring 2018. After ground warming on March 20–21 and April 20–24, 2019, ground cooling was observed, because the spring was colder than in the previous year. In both winters, seasonally frozen ground to a depth of 1.25 m persisted until mid-June in 2018 and early July in 2019 (Fig. 4).

https://doi.org/10.5194/esurf-2021-41
Preprint. Discussion started: 26 May 2021

Earth Surface Dynamics Discussions
Open Access
EGU

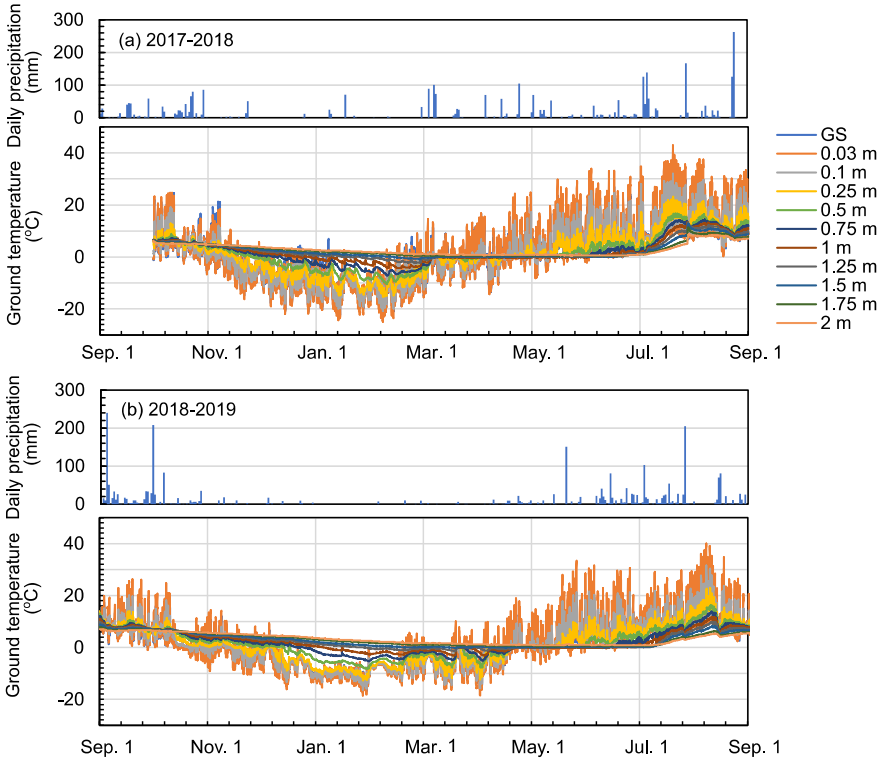

Figure 4: Temporal changes in the ground temperature at 3,220 m a.s.l. from September 1, 2017 to September 1, 2019. Daily precipitation is also shown in the figure.

https://doi.org/10.5194/esurf-2021-41
Preprint. Discussion started: 26 May 2021

Earth Surface Dynamics Discussions
Open Access
EGU

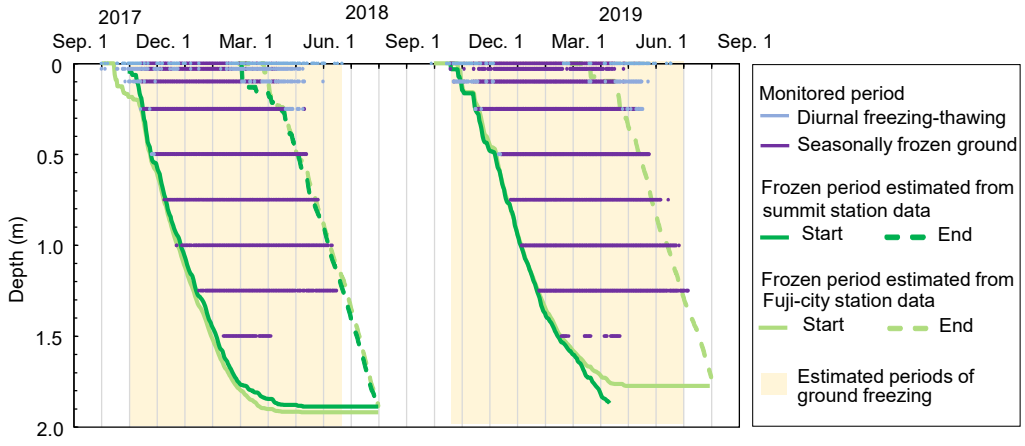

Figure 5: Comparison of observed and estimated periods of diurnal freeze-thaw activity and seasonal ground freezing at 3,221 a.s.l. The timing of thawing in 2019 could not be estimated using data from the summit station due to monitoring equipment failure. Periods of ground freezing were estimated using summit station data, whereas the end of the frozen period in 2019 was estimated using data from the Fuji City station.

The most appropriate coefficient c_f that could adequately replicate the downward progress of the freezing line was 5.5 (Fig. 5). Except in the near-surface (≤0.25 m) and deep layers (>1.5 m), positions of the freezing front were estimated based on air temperatures measured at the summit and Fuji City stations. The disagreement between the estimated freezing and observed non-freezing states at the depth of 1.75 m implied the presence of a thermal buffer, such as a layer with a high water content.

The rapid and simultaneous increase in ground temperature from negative values to the melting point (Fig. 4) indicated that thawing of the porous volcanic ground was controlled by not only heat conduction but also heat advection. Taking this into account, we calculated the coefficient c_m as an empirical value rather than a physical parameter. The empirical c_m was 6.8 when Eq. (2) best reproduced the thawing of the depths between 0.75 and 1.25 m (Fig. 5). In this study, periods of ground freezing could be roughly estimated from the time when the freezing front started to progress downward from the ground surface and the time when the estimated thawing front reached a depth of 1.25 m (Fig. 5).

4.2 Changes in channel bed topography

Channel bed topography clearly changed with time and was affected by the sediment supply from hillslopes and the evacuation of channel deposits by debris flows (Fig. 6). From September 2013 to October 2014 (Fig. 6a), no debris flow was monitored at the observatories. During this period, aggradation of the channel bed of up to 5 m in association with sediment supply from the surrounding hillslopes was evident. From September to November of 2011, the channel deposit zone was significantly eroded by a debris flow that occurred on November 9, 2011 (Fig. 6b). During this period, debris flows occurred in some

https://doi.org/10.5194/esurf-2021-41
Preprint. Discussion started: 26 May 2021

Earth Surface Dynamics Discussions
Open Access
EGU

tributaries without any failure of the surrounding hillslopes (Fig. 6b). Sediment produced by the failure of basaltic lava outcrops was deposited just below the outcrops without evolving into a debris flow. Hence, past debris flows in the Osawa failure were mainly caused by the evacuation of channel deposits rather than the direct mobilization of landslide sediment.

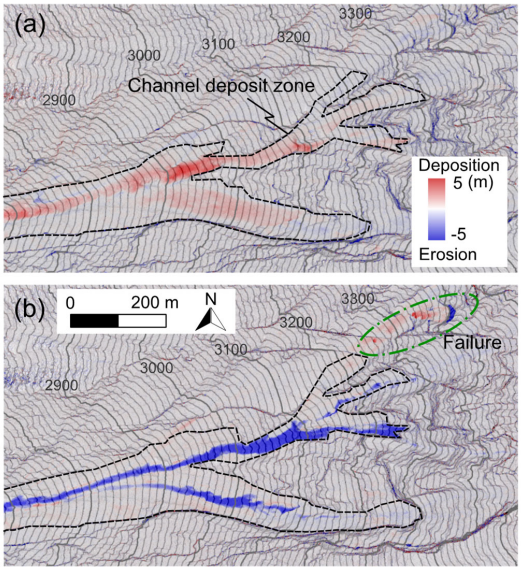

Figure 6: Changes in channel bed topography. (a) From September 2013 to October 2014, no debris flow was observed. (b) From September to November of 2011, a debris flow occurred on November 9, 2011. The dashed line indicates the area with channel deposits.

4.3 Effects of ground freezing on the conditions required to initiate a debris flow

Figure 7a shows the influence of rainfall intensity and duration on sediment transfer (i.e., debris flows and slush avalanches), which tended to occur during the conditions represented in the upper-right quadrant of all plots. This indicated that the magnitude of rainfall events that triggered sediment transfer was larger than that of an ordinary rainfall event. However, the distributions of rainfall events that did or did not trigger sediment transfer could not be completely separated. The CSI for the ID threshold was significantly low (0.21). When ID diagrams were plotted for the frozen and unfrozen periods, respectively, the distribution of rainfall events that triggered sediment transfer during frozen periods was positioned further to the lower-left side than in the corresponding diagram for unfrozen periods (Figs. 7b, 7c). Thus, the ID threshold in frozen periods was lower than that in unfrozen periods. The CSI values of the ID thresholds in the frozen and unfrozen periods were 0.42 and 0.15, respectively. Therefore, the CSI in frozen periods was substantially improved compared to the CSI for all periods. Slush

https://doi.org/10.5194/esurf-2021-41
Preprint. Discussion started: 26 May 2021

avalanches were observed only during frozen periods. Although the distribution of slush avalanches overlapped with that of debris flows, all slush avalanche events were represented on the lower left side of the threshold line.

Rainfall thresholds for the occurrence of sediment transfer were also obtained by comparing total rainfall and maximum hourly rainfall intensity (Fig. 7d). The total rainfall and maximum rainfall intensity that produced the highest CSI value were 314 mm and 42 mm h^{-1}, respectively. However, the distributions of rainfall events that did or did not trigger sediment transfer could not be completely separated (CSI = 0.15). As with the ID diagrams, rainfall events in the frozen and unfrozen periods were plotted separately (Figs. 7e, 7f). In frozen periods, the threshold values of total rainfall and maximum hourly rainfall were 120 mm and 22 mm h^{-1}, respectively. In unfrozen periods, the threshold values of total rainfall and maximum hourly rainfall were higher than those in the frozen periods (314 mm and 42 mm h^{-1}, respectively). Both of the debris flows triggered by a maximum hourly rainfall <30 mm in unfrozen periods occurred within the 10-day period prior to the estimated subsequent frozen period. Thus, it is possible that the ground was frozen when these debris flows occurred. The CSI values of the rainfall thresholds in the frozen and unfrozen periods (0.38 and 0.27, respectively) were better than that obtained using all rainfall events (0.15).

https://doi.org/10.5194/esurf-2021-41
Preprint. Discussion started: 26 May 2021

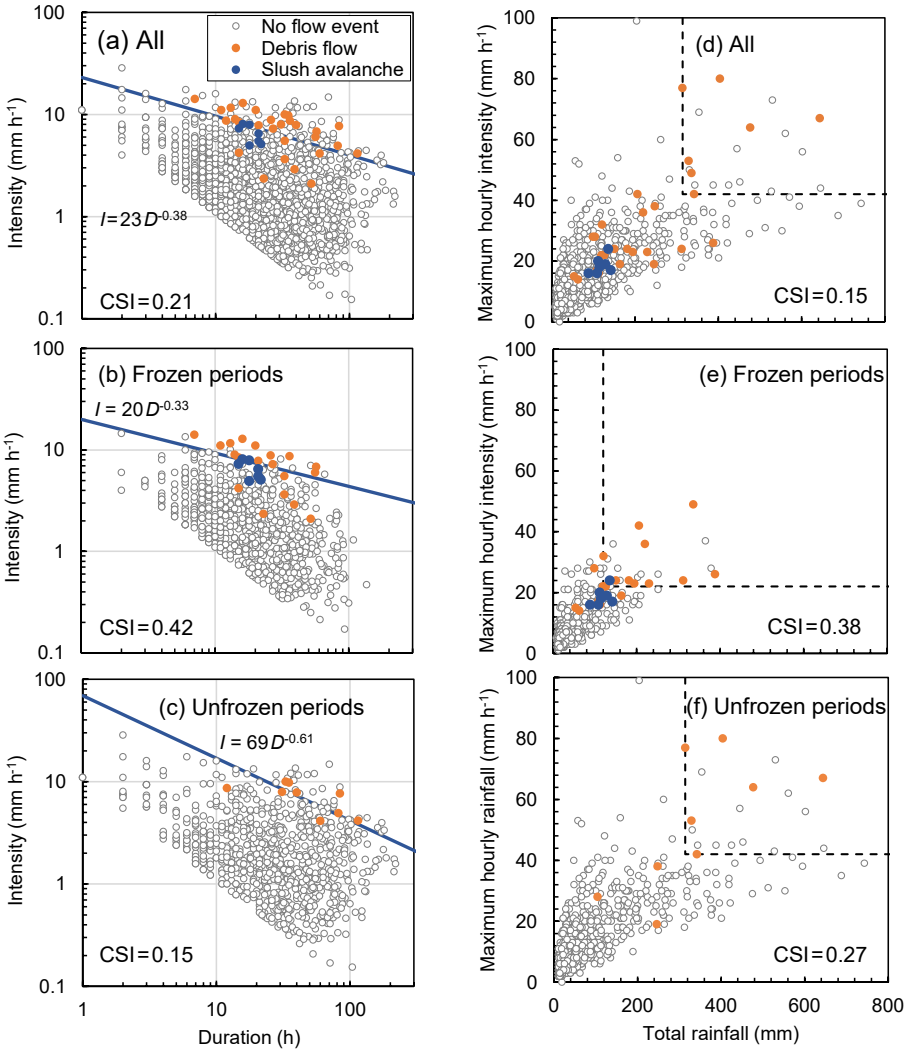

Figure 7: Rainfall thresholds for triggering debris flows and slush avalanches. Comparison of the duration and intensity of rainfall events with or without debris flows and slush avalanches for (a) all rainfall events, (b) rainfall events in frozen periods, and (c) rainfall events in unfrozen periods. Blue lines in the plots indicate the rainfall threshold, which optimally separated rainfall events that induced debris flows and slush avalanches and those that did not. Comparison of the total rainfall and the maximum hourly rainfall intensity of rainfall events with or without debris flows and slush avalanches for (d) all rainfall events, (e) rainfall events in

https://doi.org/10.5194/esurf-2021-41
Preprint. Discussion started: 26 May 2021

Earth Surface Dynamics Discussions
Open Access
EGU

frozen periods, and (f) rainfall events in unfrozen periods. Dashed lines in the plots indicate the rainfall threshold, which optimally separated rainfall events that induced debris flows and slush avalanches and those that did not.

4.4 Effects of the volume of channel deposits on the conditions required to initiate a debris flow

During frozen periods, the ID threshold was not very different between periods with large and small volumes of channel deposits (Fig. 8). The CSI values of the thresholds for small and large volumes of channel deposits were 0.45 and 0.38, respectively. Therefore, the CSI was not improved from when the ID threshold was determined without considering the volume of channel deposits (0.42, Fig. 7b). During unfrozen periods, the ID threshold in periods with a large volume of channel deposits was clearly higher than that in periods with a small volume of channel deposits (Fig. 8b). The CSI values for both volume groups (0.20 and 0.14 for small and large volumes of channel deposits, respectively) were not significantly higher than the value obtained without considering the volume of channel deposits (0.15, Fig. 7c).

As with the ID threshold, the maximum hourly intensity and total rainfall that triggered debris flows were not clearly affected by the volume of channel deposits during the frozen periods (Figs. 9a, 9b, Table 2). By contrast, the thresholds in the unfrozen periods were very different and were dependent on the volume of channel deposits (Figs. 9c, 9d, Table 2). A larger hourly rainfall intensity and total rainfall were needed for the debris flow occurence in periods with a large volume of channel deposits. Many rainfall events that exceeded the rainfall threshold in periods with a small volume of deposits did not trigger debris flows in periods with a large volume of deposits. The CSI of the rainfall thresholds obtained separately for each sediment volume class (0.30 and 0.60 for large and small volumes of channel deposits, respectively) was improved from that calculated for all rainfall levels, regardless of the sediment volume (0.27, Fig. 7f).

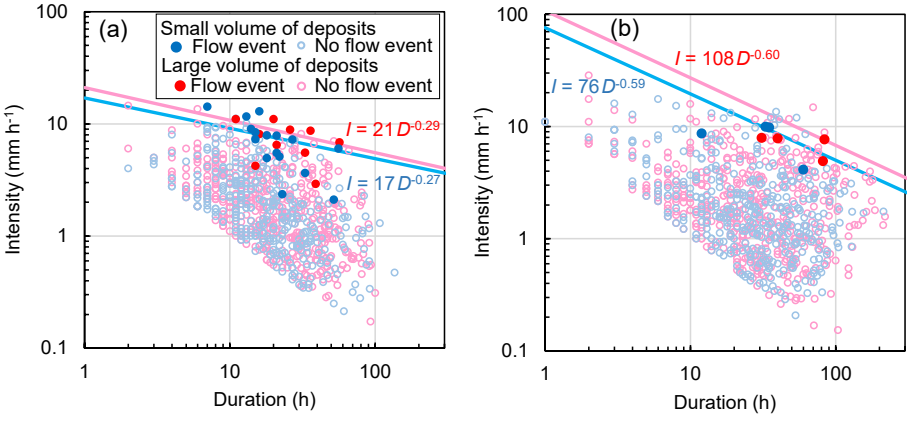

https://doi.org/10.5194/esurf-2021-41
Preprint. Discussion started: 26 May 2021

Earth Surface Dynamics Discussions
Open Access
EGU

Figure 8: Comparison of the duration and intensity of rainfall events with or without debris flows and slush avalanches, analyzed according to the volume of channel deposits. The boundary between the two volume classes was set to 350,000 m^3. (a) Frozen periods. (b) Unfrozen periods.

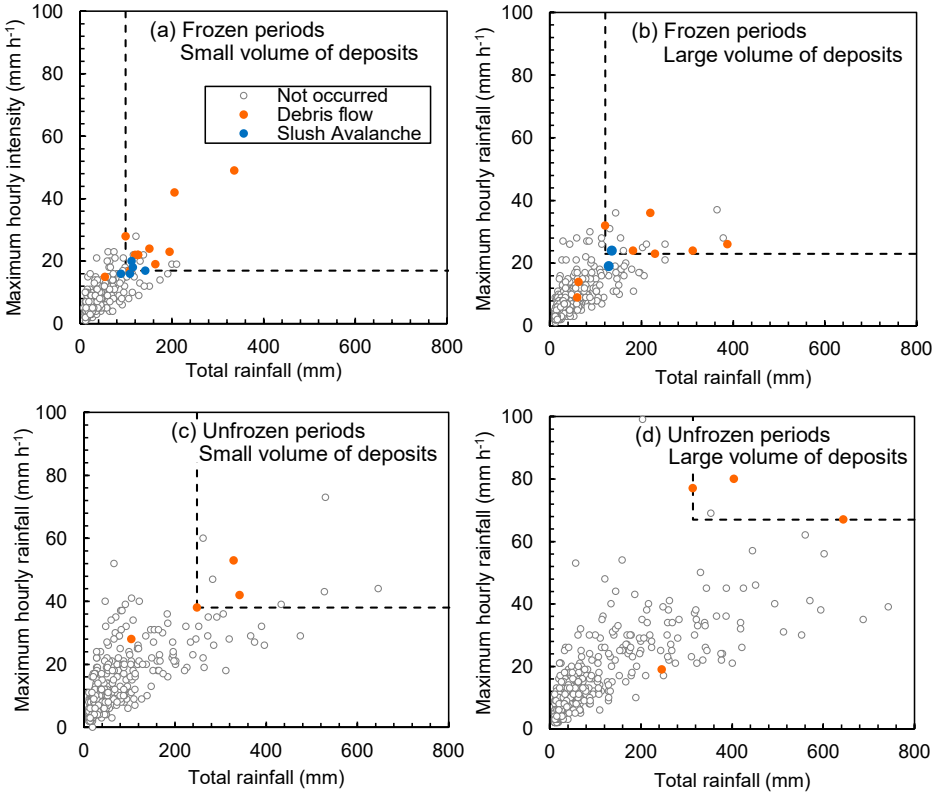

Figure 9: Comparison of total rainfall and maximum hourly rainfall in rainfall events with or without debris flows and slush avalanches, plotted according to the volume class of channel deposits. (a) Frozen periods with a small volume of deposits (<350,000 m^3). (b) Frozen periods with large volume of deposits (≥350,000 m^3). (c) Unfrozen periods with a small volume of deposits. (d) Unfrozen periods with a large volume of deposits. Dashed lines in the plots indicate rainfall thresholds, which optimally separate rainfall events that induced debris flows and slush avalanches and those that did not. The values of the rainfall thresholds are listed in Table 1.

https://doi.org/10.5194/esurf-2021-41
Preprint. Discussion started: 26 May 2021

345 **Table 2: Rainfall thresholds for triggering debris flows and slush avalanches, obtained via comparisons of maximum hourly rainfall intensity and total rainfall.**

Conditions	Number of rainfall events	Number of debris flows and slush avalanches	Rainfall threshold		CSI
			Maximum hourly rainfall (mm h^{-1})	Total rainfall (mm)	
Frozen / small volume of deposits	342	16	17	99	0.43
Frozen / large volume of deposits	460	10	23	121	0.37
Unfrozen / small volume of deposits	377	4	38	248	0.30
Unfrozen / large volume of deposits	457	4	67	314	0.60

5. Discussion

Our simple model could roughly reproduce the period of ground freezing at site TM (Fig. 5), although subsurface heterogeneity, 350 infiltration of rainfall, and upward movement of sensible heat were not considered in the model. The snowpack, which affects the period of ground freezing in many cold regions (e.g., Zhang, 2005; Luo, 2018), was not considered important to the formation of frozen ground at the monitoring point, because diurnal changes in the ground surface temperature (Fig. 4) indicated that the snowpack was never sufficiently deep to prevent ground cooling in the observed winters. The shallow snow depth in winter due to the strong wind and steep topography around the Osawa failure likely resulted in the limited influence 355 of the snowpack on the period of ground freezing.

The rainfall threshold was significantly different between the frozen and unfrozen periods (Fig. 7). Therefore, the formation of frozen ground is a critical factor affecting the initiation of a debris flow. Bovis and Dagg (1988) implied that the hydraulic conductivity of channel deposits affects temporal changes in debris flow activity. Based on constant head permeability tests in the laboratory, Nanzaka and Iwata (1989) reported that the hydraulic conductivity of frozen deposits in the Osawa failure (3 360 to 22 mm h^{-1}) was lower than that of unfrozen deposits (720 mm h^{-1}). Decreases in the infiltration rate due to ground freezing, which result in the occurrence of overland flow, have been reported in other regions (Blackburn et al., 1990; Iwata et al., 2010; Coles and McDonell, 2018). Consequently, the generation of overland flow affected by the low infiltration rate of deposits in frozen periods likely resulted in the debris flow occurence during smaller rainfall events (Fig. 7). The effect of the volume of channel deposits on the rainfall threshold was unclear in the frozen periods (Figs. 8, 9), suggesting that debris flows in these 365 periods were triggered by hydrological processes near the ground surface rather than the saturation of entire channel deposits (Fig. 10a). Increasing in the debris flow frequency due to decreasing in the infiltration rate has also been reported in the regions affected by wild fire (Staley et al., 2017; McGuire et al., 2018; Rengers et al., 2020). Because a rainfall index representing the total water supply to the basin (i.e., total rainfall) was also an important factor in the triggering of debris flows (Fig. 7e), a sufficient amount of stream discharge may also be needed for the occurrence of debris flow.

https://doi.org/10.5194/esurf-2021-41
Preprint. Discussion started: 26 May 2021

As with the Osawa failure, slush avalanches and debris flows have been recorded in other cold regions (Decaulne and Saemundsson, 2006; Decaulne, 2007). In contrast to a debris flow, the presence of a snowpack is necessary for the occurrence of a slush avalanche (Decaulne, 2007; Eckerstorfer and Christiansen, 2012). The magnitude of rainfall events triggering slush avalanches were smaller than those that triggered debris flows (Fig. 7). Because snow in a slush avalanche sometimes melts as it moves to lower elevations due to the increasing temperature (Anma, 2007), some sediment transfer events classified as debris flow would originally be slush avalanches in the initiation zone. That could be one of the reasons why the distributions of slush avalanches and debris flows according to rainfall factors overlapped in Fig. 7.

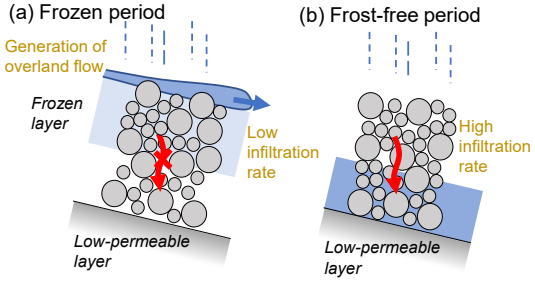

Figure 10: Schematic diagram of the hydrological characteristics of the Osawa failure. (a) Frozen periods. (b) Unfrozen periods.

In contrast to the frozen periods, overland flow rarely occurred in the unfrozen periods because of the high infiltration rate of the deposits. Therefore, an increase in the groundwater level in channel deposits would likely influence the occurrence of debris flows (Fig. 10b). The slope of the ID threshold in environments in which the rainfall duration was important was steeper than in environments in which rainfall intensity was important (Guzzetti et al., 2008). A steeper threshold line in the unfrozen periods relative to the frozen periods (Fig. 8) indicated that rainfall duration was the important factor in the unfrozen periods. A large rainfall magnitude was needed for the occurrence of debris flows when a large volume of sediment was stored in the initiation zone (Figs. 8, 9). The relationship between the rainfall threshold and the volume of sediment stored was different from that reported in weathering-limited debris flow basins (Bovis and Jakob, 1999; Larsen et al., 2006). Because debris flows occurred even in periods with a small volume of channel deposits (Fig. 3), the threshold of sediment volume needed for the occurrence of a debris flow, which has been reported in weathering-limited basins (Bovis and Jakob, 1999), was not clear in the Osawa failure. The relationship between the rainfall threshold and the storage volume in the Osawa failure was also different from that in transport-limited basins, in which the rainfall threshold can be given as a constant value regardless of the storage volume (Bovis and Jakob, 1999; Schlunegger et al., 2009). Channel deposits in the Osawa failure had a thickness of up to 10 m in some periods and were also characterized by a high infiltration rate. The ratio of thickness of the saturated layer to the entire thickness of the deposits is a factor controlling the movement of cohesionless deposits in steep channels (Imaizumi

https://doi.org/10.5194/esurf-2021-41
Preprint. Discussion started: 26 May 2021

et al., 2016, 2017). A large water supply is needed for the movement of thick deposits. Hence, the volume of channel deposits likely has a negative effect on the debris flow occurence in unfrozen periods.

Plots of rainfall events with and without debris flow events overlapped to a certain extent, even after consideration of the frozen periods and volume of channel deposits (Figs. 8, 9). The magnitude of some rainfall events that triggered debris flows in unfrozen periods was as low as those in the frozen periods (Fig. 7), indicating that it is difficult to accurately estimate when frozen periods occur. Because periods of ground freezing differ with slope aspect and elevation, it was difficult to determine if the ground was frozen at the initiation point for all events. Another potential factor reducing the CSI was the spatial variability of precipitation in the Osawa failure, which has a difference of elevation of up to 1,500 m. The ID threshold for the Osawa failure was higher than those measured for many other torrents globally (e.g., Guzzetti et al., 2008; Bezak et al., 2016; Hürlimann et al., 2019). Although the lower limit for debris flow in the Osawa failure was not far from the ID thresholds for other regions, rainfall levels above the lower limit without the debris flow occcurence pushed the threshold upward. In general, the lower-limit lines for debris flow are lower than the lines separating rainfall events with and without debris flows (Cannon et al., 2008; Bezak et al., 2016). Because the debris flow threshold is often the lower-limit line (Cannon et al., 2008; Guzzetti et al., 2008), the threshold in the Osawa failure gully is higher. The observatories are located far from the debris flow initiation zone, resulting in debris flows just a short distance away being missed. This might have also affected the higher threshold line.

6. Summary and Conclusion

To determine the effects of frozen ground on temporal changes in the rainfall threshold for the occurrence of debris flows and slush avalanches, we estimated periods of seasonal ground freezing based on field monitoring conducted close to the initiation zone in the Osawa failure on Mt. Fuji. We also evaluated the influence of sediment storage volume in the debris flow initiation zone on the rainfall threshold. The ID threshold in periods of ground freezing was clearly lower than in periods without ground freezing. A comparison of the maximum hourly rainfall intensity and total rainfall during rainfall events also showed that debris flows occurred during periods of seasonal ground freezing with rainfall events of a smaller magnitude. Decreases in the infiltration rate due to the formation of frozen ground facilitated the generation of overland flow, which triggered debris flows.

The volume of channel deposits also affected the rainfall threshold, especially during unfrozen periods. The rainfall threshold in periods with large volumes of channel deposits was higher than that in periods with small volumes of channel deposits, indicating that a large water supply is needed for the debris flow occurrence when channel deposits are thick. Increases in the water content in channel deposits caused by the infiltration of rainfall are important for the debris flow occurence during unfrozen periods, whereas hydrological processes near the ground surface are more important in frozen periods.

Our study determined that the rainfall threshold is variable even in the same torrent due to the influence of the formation of frozen ground and changes in sediment storage volume. Therefore, the occurrence of frozen ground and the sediment storage

https://doi.org/10.5194/esurf-2021-41
Preprint. Discussion started: 26 May 2021

volume need to be monitored and estimated to improve debris flow disaster mitigation in cold regions. Because periods of ground freezing and the sediment supply ratio are strongly affected by climatic conditions, future changes in the debris flow threshold should be carefully monitored for continuous sediment flow-associated disaster mitigation under climate change.

Data availability

The data that support the findings of this study are available from the corresponding author, Fumitoshi Imaizumi, upon reasonable request and agreement by Ministry of Land, Infrastructure, Transport and Tourism, Japan.

Author contributions

FI and OO conceived and designed the study. AI designed and conducted field monitoring of ground freezing. KY contributed analyses of historical rainfall data. All of the authors conducted field motoring. FI contributed to the writing of the paper.

Competing interests

The authors declare that they have no conflict of interest

Acknowledgements

This study was funded by Ministry of Land, Infrastructure, Transport and Tourism, Japan. This study was also supported by by JSPS Grant Numbers 18H02235 and 19K01156. Airborne DEMs and rainfall data was provided by Fuji Sabo Office, Chubu Regional Bureau, Ministry of Land, Infrastructure, Transport and Tourism, Japan.

References

Anma, S.: Lahars and Slush Lahars on the Slopes of Fuji Volcano. Aramaki et al. Ed., Fuji Volcano, 285–301 (in Japanese with English abstract), 2007.

Bayard, D., Stähli, M., Parriaux, A., and Flühler, H: The influence of seasonally frozen soil on the snowmelt runoff at two Alpine sites in southern Switzerland, J. Hydrol., 309, 66–84. https://doi.org/10.1016/j.jhydrol.2004.11.012, 2005

Berger, C., McArdell, B. W., and Schlunegger, F.: Sediment transfer patterns at the Illgraben catchment, Switzerland: Implications for the time scales of debris flow activities, Geomorphology, 125, 421–432. https://doi.org/10.1016/j.geomorph.2010.10.019, 2011

https://doi.org/10.5194/esurf-2021-41
Preprint. Discussion started: 26 May 2021

Blackburn, W. H., Pierson, F. B., and Seyfried, M. S.: Spatial and temporal influence of soil frost on infiltration and erosion of sagebrush rangeland. J. Am. Water Res. As., 26(6), 991–997. https://doi.org/10.1111/j.1752-1688.1990.tb01434.x, 1990.

Bovis, M. J., and Jakob, M.: The roll of debris supply conditions in predicting debris flow activity, Earth Surf. Process. Landf., 24, 1039–1054. https://doi.org/10.1002/(SICI)1096-9837(199910)24:11<1039::AID-ESP29>3.0.CO;2-U, 1999.

Bovis, M.J. and Dagg, B. R.: A model for debris accumulation and mobilization in steep mountain streams, Hydrol. Sci. J., 33, 589–604, 1988.

Caine, N.: The rainfall intensity–duration control of shallow landslides and debris flows, Geogr. Ann. A 62, 23–27, 1980.

Cannon, S. H., Kirkham, R. K., and Parise, M.: Wildfire-related debris-flow initiation processes, Storm King Mountain, Colorado, Geomorphology, 39, 171–188, https://doi.org/10.1016/S0169-555X(00)00108-2, 2001.

Cannon S. H., Boldt, E. M., Laber, J.L., Kean, J.W., and Staley, D. M.: Rainfall intensity-duration thresholds for postfire debris-flow emergency-response planning, Nat. Hazards, 59, 209–236, https://doi.org/10.1007/s11069-011-9747-2, 2011.

Chen, H. X., Zhang, L. M., Chang, D. S., and Zhang, S.: Mechanisms and runout characteristics of the rainfall triggered debris flow in Xiaojiagou in Sichuan Province, China, Nat. Hazards, 62, 1037–1057. https://doi.org/10.1007/s11069-012-0133-5, 2012.

Coles, A. E., and McDonnell, J. J.: Fill and spill drives runoff connectivity over frozen ground, J. Hydrol., 558, 115–128. https://doi.org/10.1016/j.jhydrol.2018.01.016, 2018.

Decaulne, A.: Snow-avalanche and debris-flow hazards in the fjordsof north-western Iceland, mitigationand prevention, Nat. Hazards, 41, 81–98. https://doi.org/10.1007/s11069-006-9025-x, 2007.

Ebel, B. A., Moody, J. A., and Martin, D. M.: Hydrologic conditions controlling runoff generation immediately after wildfire. Water Resour. Res., 48, W03529, https://doi.org/10.1029/2011WR011470, 2012

Decaulne, A., and Saemundsson, T.: Geomorphic evidence for present-day snow-avalanche and debris-flow impact in the Icelandic Westfjords. Geomorphology, 80, 80–93, https://doi.org/10.1016/j.geomorph.2005.09.007, 2006.

Eckerstorfer, M., and Christiansen, H. H.: Meteorology, topography and snowpack donditions causing two extreme mid-winter slush and wet slab avalanche periods in high Arctic maritime Svalbard. Permafr. Periglac. Process., 23, 15–25, https://doi.org/10.1002/ppp.734, 2012.

Fiollio, F., and Wilson, R. C.: Rainfall induced debris flows in pyroclastic deposits, Campania (southern Italy), Eng. Geol. 75, 263–289, https://doi.org/10.1016/j.enggeo.2004.06.014, 2004.

Fuji Sabo Office: Monitoring reports of sediment transport monitoring at Mt. Fuji in 2016 financial year, Fuji Sabo Office, Ministry of Land, Infrastructure, Transport and Tourism, Japan (in Japanese), 2017.

Fuji Sabo Office: Monitoring reports of sediment transport monitoring at Mt. Fuji in 2019 financial year, Fuji Sabo Office, Ministry of Land, Infrastructure, Transport and Tourism, Japan (in Japanese), 2020.

Formetta, G., Capparelli, G., and Versace, P.: Evaluating performance of simplified physically basedmodels for shallow landslide susceptibility, Hydrol. Earth Syst. Sci., 20, 4585–4603, https://doi.org/10.5194/hess-20-4585-2016, 2016.

https://doi.org/10.5194/esurf-2021-41
Preprint. Discussion started: 26 May 2021

485 Guzzetti, F, Peruccacci, S, Rossi, M, and Stark, CP: The rainfall intensity–duration control of shallow landslides and debris flows: an update, Landslides, 5, 3–17, https://doi.org/10.1007/s10346-007-0112-1, 2008.

Dowling, C. A., and Santi, P.: Debris flows and their toll on human life: a global analysis of debris-flow fatalities from 1950 to 2011, Nat. Hazards, 71, 203–227, https://doi.org/10.1007/s11069-013-0907-4, 2014.

Hanaoka, M., Tomita, Y., and Ito, M.: Osawa Kuzure (failure) and debris flows in Mt. Fuji, Aramaki et al. Ed., Fuji Volcano,
490 407–425 (in Japanese with English abstract), 2007.

Hürlimann, M., Coviello, V., Bel, C., Guo, X., Berti, M., Graf, C., Hübl, J., Miyata S., Smith, J. B., and Yin, H. Y.: Debris-flow monitoring and warning: Review and examples, Earth-Sci. Rev., 199, 102981, https://doi.org/10.1016/j.earscirev.2019.102981, 2019.

Imaizumi, F., Hayakawa, Y.S., Hotta, N., Tsunetaka, H., Ohsaka, O., and Tsuchiya, S.: Relationship between the accumulation
495 of sediment storage and debris-flow characteristics in a debris-flow initiation zone, Ohya landslide body, Japan, Nat. Hazards Earth Syst. Sci., 17, 1923–1938. https://doi.org/10.5194/nhess-17-1923-2017, 2017.

Imaizumi, F., Sidle, R. C., Tsuchiya, S., and Ohsaka, O.: Hydrogeomorphic processes in a steep debris flow initiation zone. Geophys. Res. Lett., 33, L10404, https://doi.org/10.1029/2006GL026250, 2006.

Imaizumi F., Tsuchiya, S., and Ohsaka, O.: Field observations of debris-flow initiation processes on sediment deposits in a
500 previous deep-seated landslide site, J. Mount. Sci, 13, 213–222, https://doi.org/10.1007/s11629-015-3345-9, 2016.

Imaizumi, F., Masui, T., Yokota, Y., Tsunetaka, H., Hayakawa, Y.S., and Hotta, N.: Initiation and runout characteristics of debris flow surges in Ohya landslide scar, Japan, Geomorphology, 339, 58-69, https://doi.org/10.1016/j.geomorph.2019.04.026, 2019.

Iwata, Y., Hayashi, M., Suzuki, S., Hirota, T., and Hasegawa, S.: Effects of snow cover on soil freezing, water movement, and
505 snowmelt infiltration: A paired plot experiment, Water Resour. Re., 46, W09504, https://doi.org/10.1029/2009WR008070, 2010.

Iwatsuka, S., and Machida, H.: The development of Osawa Valley, Mt. Fuji —The fundamental study on the Development of radial valleys on Volcano—, J. Geogr. (Chigaku Zasshi), 729, 3–18 (in Japanese with English abstract). https://doi.org/10.5026/jgeography.71.143, 1962.

510 Jakob, M., Bovis, M., and Oden, M.: The significance of channel recharge rates for estimating debris-flow magnitude and frequency. Earth Surf. Process. Landf., 30, 755–766, https://doi.org/10.1002/esp.1188, 2005.

Kneisel, C., Emmert, A., Polich, P., Zollinger, B., and Egli M.: Soil geomorphology and frozen ground conditions at a subalpine talus slope having permafrost in the eastern Swiss Alps, Catena, 133, 107–118, https://doi.org/10.1016/j.catena.2015.05.005, 2015.

515 Larsen, I. J., Pederson, J. L., and Schmidt, J. C.: Geologic versus wildfire controls on hillslope processes and debris flow initiation in the Green River canyons of Dinosaur National Monument, Geomorphology, 81, 114–127, https://doi.org/10.1016/j.geomorph.2006.04.002, 2006.

https://doi.org/10.5194/esurf-2021-41
Preprint. Discussion started: 26 May 2021

Liao, Z. H., Hong, Y., Kirschbaum, D., Adler, R. F., Gourley, J. J., and Wooten, R.: Evaluation of TRIGRS (transient rainfall infiltration and grid-based regional slope-stability analysis)'s predictive skill for hurricane-triggered landslides: a case study in Macon County, North Carolina. Nat. Hazards, 58, 325–339. https://doi.org/10.1007/s11069-010-9670-y, 2011.

Loye, A., Jaboyedoff, M., Theule, J. I., and Liébault, F.: Headwater sediment dynamics in a debris flow catchment constrained by high-resolution topographic surveys, Earth Surf. Dynam., 4, 489–513, https://doi.org/10.5194/esurf-4-489-2016, 2016.

Luo, D., Jin, H., Marcheko, S. S., and Romanovsky, V E.: Difference between near-surface air, land surface and ground surface temperatures and their influences on the frozen ground on the Qinghai-Tibet Plateau. Geoderma, 312, 74–85, https://doi.org/10.1016/j.geoderma.2017.09.037, 2018.

May, C. L.: Debris flows throughout different forest age classes in the central Oregon coast range, J. A. Water. Resour. As. 38, 1097–1113. https://doi.org/10.1111/j.1752-1688.2002.tb05549.x, 2002.

McGuire, L. A., Rengers, F. K., Kean, J. W., Staley, D. M., and Mirus, B. B.: Incorporating spatially heterogeneous infiltration capacity into hydrologic models with applications for simulating post-wildfire debris flow initiation. Hydrol. Process., 32, 1173–1187, https://doi.org/10.1002/hyp.11458, 2018.

Miao, Y., Shi, Y., Zhuang, H. Y., Wang, S. Y., and Liu, H. B.: Influence of Seasonal Frozen Soil on Near-Surface Shear Wave Velocity in Eastern Hokkaido, Japan, Geophys. Res. Lett., 46, 9497–9508, https://doi.org/10.1029/2019GL082282, 2019.

Miyaji, N.: Histories of younger Fuji volcano, J. Geol. Soc. of Japan, 94, 433–452 (in Japanese with English abstract), 1988.

Nanzaka, J., and Iwata, Y.: Debris flow and frozen soil layer at the Osawa collapse in Mt. Fuji, J. Japan Soc. Eros. Control Eng., 42(4), 23-27 (in Japanese), https://doi.org/10.11475/sabo1973.42.4_23, 1989.

Pan H. L., Jiang, Y. J., Wang, J., and Ou G. Q.: Rainfall threshold calculation for debris flow early warning in areas with scarcity of data, Nat. Hazards Earth Syst. Sci., 18, 1395–1409, https://doi.org/10.5194/nhess-18-1395-2018, 2018.

Rengers, F. K., McGuire, L. A., Oakley, N. S., Kean, J. W., Staley, D. M., and Tang, H.: Landslides after wildfire: initiation, magnitude, and mobility. Landslides, 17, 2631–2641, https://doi.org/10.1007/s10346-020-01506-3, 2020.

Sidle, R. C., and Chigira, M.: Landslides and debris flows strike Kyushu, Japan, EOS, 85, 145–151. https://doi.org/10.1029/2004EO150001, 2011.

Schlunegger, F., Badoux, A., McArdell, B. W., Gwerder, C., Schnydrig, D., Rieke-Zapp, D., and Molnar, P.: Limits of sediment transfer in an alpine debris-flow catchment, Illgraben, Switzerland, Quat. Sci. Rev., 28, 1097–1105. https://doi.org/10.1016/j.quascirev.2008.10.025, 2009.

Scott, K. M., Vallance, J. W., Kerle, N., Luis Macías, J., Strauch, W., and Devoli, G.: Catastrophic precipitation-triggered lahar at Casita volcano, Nicaragua: occurrence, bulking and transformation, Earth Surf. Process. Landf., 30, 59–79, https://doi.org/10.1002/esp.1127, 2014.

Shakesby R. A., and Doerr S. H.: Wildfire as a hydrological and geomorphological agent, Earth-Sci. Rev., 74, 269–307, https://doi.org/10.1016/j.earscirev.2005.10.006, 2006.

Shanley, J. B, and Chalmers, A.: The effect of frozen soil on snowmelt runoff at Sleepers River, Vermont, Hydrol. Process., 13, 1843–1857. https://doi.org/10.1002/(SICI)1099-1085(199909)13:12/13<1843::AID-HYP879>3.0.CO;2-G, 1999.

https://doi.org/10.5194/esurf-2021-41
Preprint. Discussion started: 26 May 2021

Song, D., Zhou, G. G. D., Xu, M., Choi, C. E., Li, S., and Zheng, Y.: Quantitative analysis of debris-flow flexible barrier capacity from momentum and energy perspectives, Eng. Geol., 251, 81–92, https://doi.org/10.1016/j.enggeo.2019.02.010, 2019.

Staley, D. M., Kean, J. W., Cannon, S. H., Schmidt, K. M., and Laber, J. L.: Objective definition of rainfall intensity–duration thresholds for the initiation of post-fire debris flows in southern California, Landslides, 10, 547–562, https://doi.org/10.1007/s10346-012-0341-9, 2012.

Staley, D. M., Wasklewicz, T. A., Kean, J. W.: Characterizing the primary material sources and dominant erosional processes for post-fire debris-flow initiation in a headwater basin using multi-temporal terrestrial laser scanning data. Geomorphology, 214, 324–338, https://doi.org/10.1016/j.geomorph.2014.02.015, 2014.

Staley, D. M., Negri, J. A., Kean, J. W., Laber, J. L., Tillery, A. C., and Youberg, A. M.: Prediction of spatially explicit rainfall intensity–duration thresholds for post-fire debris-flow generation in the western United States. Geomorphology, 278, 149–162, https://doi.org/10.1016/j.geomorph.2016.10.019, 2017.

Stoffel, M, Huggel, C: Effects of climate change on mass movements in mountain environments. Prog. in Phys. Geogr., 36, 421–439, https:// 10.1016/j.scitotenv.2014.02.102, 2012.

Stoffel, M., Mendlik, T., Schneuwly-Bollschweiler, M., and Gobiet A.: Possible impacts of climate change on debris-flow activity in the Swiss Alps, Clim. Change, 122, 141–155, https://doi.org/10.1007/s10584-013-0993-z, 2014

Theule, J. I., Li´ebault1, F., Loye, A., Laigle1, D., and Jaboyedoff, M.: Sediment budget monitoring of debris-flow and bedload transport in the Manival Torrent, SE France, Nat. Hazards Earth Syst. Sci., 12, 731–749, https://doi.org/10.5194/nhess-12-731-2012, 2012.

Theule, J. I., Crema, S., Marchi, L., Cavalli, M., and Comiti, F.: Exploiting LSPIV to assess debris-flow velocities in the field, Nat. Hazards Earth Syst. Sci., 18, 1–13, https://doi.org/10.5194/nhess-18-1-2018, 2018.

Yamazaki, T., Nishida, A., & Kondo, J.: Seasonal frost depth of ground with the bare surface, snow cover and vegetation, J. Japan. Soc. Snow Ice, 60(3), 213–224, https://doi.org/10.5331/seppyo.60.213 (in Japanese), 1998.

Walvoord M. A., Voss, C. I., Ebel, E. A., and Minsley, B. J.: Development of perennial thaw zones in boreal hillslopes enhances potential mobilization of permafrost carbon, Environ, Res. Lett., 14, 015003, https://doi.org/10.1088/1748-9326/aaf0cc, 2019.

Zhang, T.: Influence of the seasonal snow cover on the ground thermal regime: An overview, Rev. Geophys., 43, RG4002. https://doi.org/10.1029/2004RG000157, 2005.

Zhang, K., Wang, S., Bao, H., and Zhao, X: Characteristics and influencing factors of rainfall-induced landslide and debris flow hazards in Shaanxi Province, China, Nat. Hazards Earth Syst. Sci., 19, 93–105, 2019.

Zhou, W., and Tang, C.:Rainfall thresholds for debris flow initiation in the Wenchuan earthquake-stricken area, southwestern China, Landslides, 11, 877–887, https://doi.org/10.1007/s10346-013-0421-5, 2014.